Environmental Science & Technology

Article

pubs.acs.org/est

Identifying the Sources and Processes of Mercury in Subtropical Estuarine and Ocean Sediments Using Hg Isotopic Composition

Runsheng Yin,[†,‡] Xinbin Feng,[§] Baowei Chen,[†] Junjun Zhang,[†] Wenxiong Wang,[∥] and Xiangdong Li*[,†]

[†]Department of Civil and Environmental Engineering, The Hong Kong Polytechnic University, Hung Hom, Kowloon, Hong Kong
[‡]State Key Laboratory of Ore Deposit Geochemistry, Institute of Geochemistry, and [§]State Key Laboratory of Environmental Geochemistry, Institute of Geochemistry, Chinese Academy of Sciences, Guiyang, Guizhou 550002, People's Republic of China
[∥]Division of Life Science, The Hong Kong University of Science and Technology, Clearwater Bay, Kowloon, Hong Kong

Supporting Information

ABSTRACT: The concentrations and isotopic compositions of mercury (Hg) in surface sediments of the Pearl River Estuary (PRE) and the South China Sea (SCS) were analyzed. The data revealed significant differences between the total Hg (THg) in fine-grained sediments collected from the PRE (8−251 $\mu g\ kg^{-1}$) and those collected from the SCS (12−83 $\mu g\ kg^{-1}$). Large spatial variations in Hg isotopic compositions were observed in the SCS (δ^{202}Hg, from −2.82 to −2.10‰; Δ^{199}Hg, from +0.21 to +0.45‰) and PRE (δ^{202}Hg, from −2.80 to −0.68‰; Δ^{199}Hg, from −0.15 to +0.16‰). The large positive Δ^{199}Hg in the SCS indicated that a fraction of Hg has undergone Hg^{2+} photoreduction processes prior to incorporation into the sediments. The relatively negative Δ^{199}Hg values in the PRE indicated that photoreduction of Hg is not the primary route for the removal of Hg from the water column. The riverine input of fine particles played an important role in transporting Hg to the PRE sediments. In the deep ocean bed of the SCS, source-related signatures of Hg isotopes may have been altered by natural geochemical processes (e.g., Hg^{2+} photoreduction and preferential adsorption processes). Using Hg isotope compositions, we estimate that river deliveries of Hg from industrial and urban sources and natural soils could be the main inputs of Hg to the PRE. However, the use of Hg isotopes as tracers in source attribution could be limited because of the isotope fractionation by natural processes in the SCS.

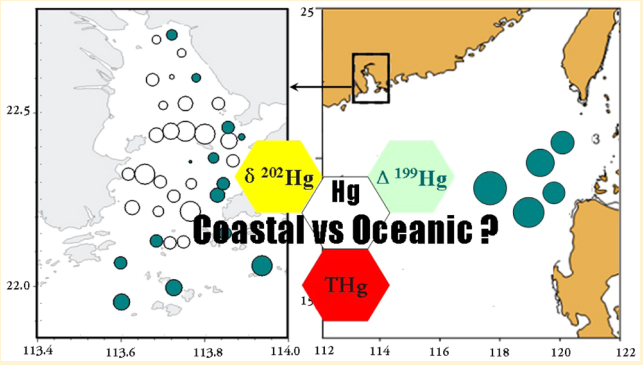

INTRODUCTION

Mercury (Hg) is known to be a toxic heavy metal that can be transported rapidly around the globe because of its high volatility and atmospheric transport.[1,2] The global open oceans play a vital role in the global cycling of Hg[2]. The global open oceans contribute about $\sim 3.0 \times 10^6$ kg $year^{-1}$ of global Hg^0 emissions to the atmosphere.[2] Meanwhile, the open oceans also receive $\sim 4.0 \times 10^6$ kg of Hg, mainly through atmospheric deposition.[2] The additional net input of Hg to the open oceans mainly comes from anthropogenic Hg emissions, which have greatly increased since the preindustrial era.[1−3] The accumulation of Hg in the marine environment (e.g., sediments) has led to a potential risk to humans or others because Hg can be easily converted into methylmercury (Me-Hg), a neurotoxin that can be biomagnified along the food chain.[3]

Estuaries are essentially biogeochemical interfaces because they link two major aqueous systems: rivers and oceans.[4] River-derived Hg can be a very important source of Hg in estuaries.[4] Benthic sediments serve as a sink for most of this river-derived Hg because most Hg in rivers is bound to particles.[5] An estimated 90% of river-derived Hg is buried in sediments at ocean margins.[5] Anthropogenic activities have resulted in Hg contamination in many estuaries, a notable example of which can be seen in the Pearl River Estuary (PRE), the largest estuary in the northern part of the South China Sea (SCS).[6−9] The PRE is surrounded by Hong Kong, Guangzhou, Macao, Shenzhen, Zhuhai, and Dongguan cities and is one of the most industrialized and urbanized regions in China.[10] During the last 3 decades, rapid economic development in the region has led to serious contamination of heavy metals (e.g., Pb, Zn, Cu, and Cr) in the PRE.[6] A large amount of Hg was used in chloralkali industries and manufacture of electrical products, alloy materials, and other goods for the global market.[11] Mercury was released by wastewater discharge and flue gas emissions, which have resulted in Hg contamination to the local environment and the adjacent ecosystems, including contamination to air, soil, water, and organisms.[7−9]

Research into Hg stable isotope biogeochemistry is offering new insight into the behavior of Mercury. Mercury has seven

Received: February 10, 2014
Revised: January 2, 2015
Accepted: January 7, 2015
Published: January 7, 2015

DOI: 10.1021/es504070y
Environ. Sci. Technol. 2015, 49, 1347−1355

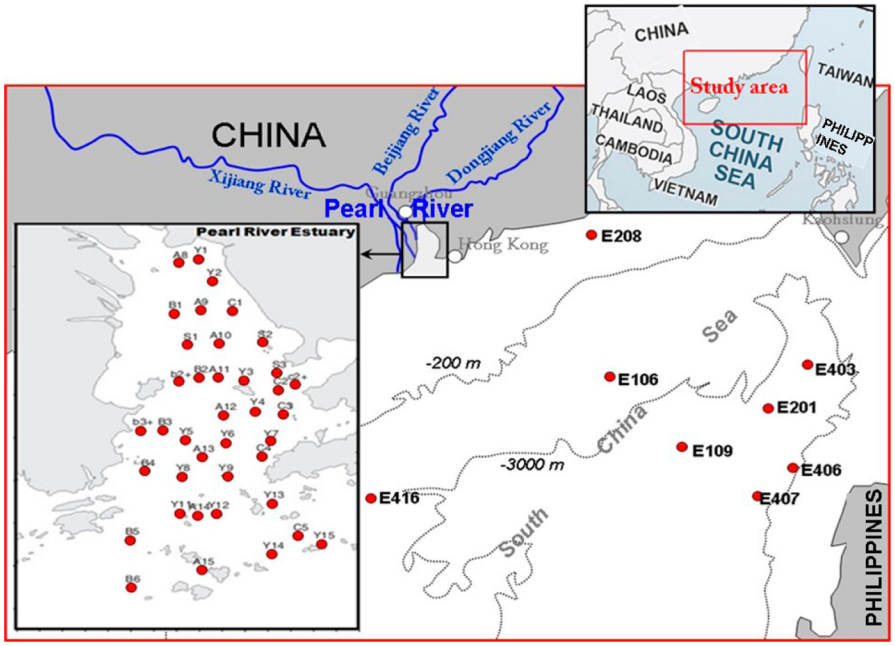

Figure 1. Study area and sampling sites.

natural stable isotopes (^{196}Hg, ^{198}Hg, ^{199}Hg, ^{200}Hg, ^{201}Hg, ^{202}Hg, and ^{204}Hg). Previous studies have demonstrated large variations in Hg isotopic composition in mineral/rock,[12−15] coal,[16,17] soil/sediment,[11,15,16,18−22] snow/precipitation,[23−25] atmosphere,[25−27] and biota.[28,29] Both mass-dependent fractionation (MDF) and mass-independent fractionation (MIF) of the Hg isotopes have been documented during various geochemical processes, such as microbial-mediated reactions (e.g., reduction,[30,31] methylation,[32] and demethylation[33]), abiotic chemical reactions (e.g., photoreduction[28,34,35] and chemical reduction[36,37]), and physical processes (e.g., volatilization,[38] evaporation,[39] adsorption,[40,41] and dissolution[42]). Hence, Hg stable isotopes have been used as an effective tool for identifying sources of Hg and tracing them through the environmental medium.[43−45]

Spatial and temporal variations in Hg isotopes in sediments have been measured in many studies to identify the sources and trace the pollution history of Hg.[11,15,46−52] On the basis of well-defined end-members with distinct Hg isotope signatures, binary and ternary mixing models have been successfully used to quantify the relative contributions of different sources of Hg in the sediments.[11,48,50,51] In 2011, in an initial study, Liu et al.[11] demonstrated large differences in Hg isotopic compositions from industrial, urban, and continental background sources of Hg in the Dongjiang River, one of the largest tributaries flowing into the PRE.[18] Later, they applied a triple mixing model to quantify the contribution of each source of Hg in the Dongjiang River sediments.[11] However, the Hg isotopic compositions of sediments in the PRE and SCS have not been explored by taking into consideration the fresh water and marine current interactions and the air and water interfaces in this dynamic coastal environment. Whether the Hg isotopic signatures identified in the upstream river sediments are present in the PRE and SCS and how Hg transforms in the estuarine and open ocean systems are questions that need to be studied.[11] Answers to these questions may increase our understanding of Hg biogeochemical cycling in the subtropical oceans of the world. Here, we conducted an investigation into the Hg isotopic composition in the surface sediments of the PRE and SCS. The objectives of this study were (1) to use Hg isotopic measurements to investigate the manner in which anthropogenic activities have altered the sources of Hg in the PRE and SCS and (2) to use Hg isotopes to understand the geochemical processes relating to Hg cycling that occur in a subtropical coastal environment.

EXPERIMENTAL SECTION

Study Area and Sampling. The SCS encompasses an area of ~3.5 × 10^6 km^2, with a mean depth of 1.212 km. The PRE is a subtropical estuary located in the northern part of the SCS (Figure 1). It covers an area of ~2000 km^2, with an average distance of 49 km from north to south and 4−58 km from east to west.[6] The depth of the PRE varies from 0 to 30 m.[53] The tides (range of 1.0−1.7 m) in the PRE mainly come from Pacific oceanic tidal propagation.[53] Surface runoffs from three major tributaries (Xijiang River, Beijiang River, and Dongjiang River) of the Pearl River bring about 326 × 10^9 m^3 year^{-1} of fresh water and 89 × 10^9 kg year^{-1} of sediment into the PRE.[6] The total suspended matter in surface water decreases from the northern PRE (>34 mg L^{-1}) to the southern PRE (<20 mg L^{-1}).[54] Much higher water clarity (Secchi disk depth) was observed in the southern PRE (4−18 m) than in the northern PRE (<1 m).[55] Surface fine-grained sediments (0−2 cm) were collected from the PRE (n = 39) in June 2011. Sediments (n = 8) were also collected in the SCS (at an average depth of >3000 m) during August 2011. All sediments were taken using a grab sampler (Van Veen grab) and immediately stored in polyethylene plastic bags. Following their collection, the sediments were freeze-dried (−50 °C for 72 h), ground, and homogenized using a mortar and pestle until the particles were <200 μm. Details of the sampling sites (e.g., location and depth) are summarized in Table S1 of the Supporting Information. The concentrations of trace metals (e.g., Co, Cr, Cu, Ni, Pb, and Zn) and major elements (e.g., Al, Fe, Mg, and Mn) as well as the concentrations of fine particles (<2 μm, represented as C_p)

DOI: 10.1021/es504070y
Environ. Sci. Technol. 2015, 49, 1347−1355

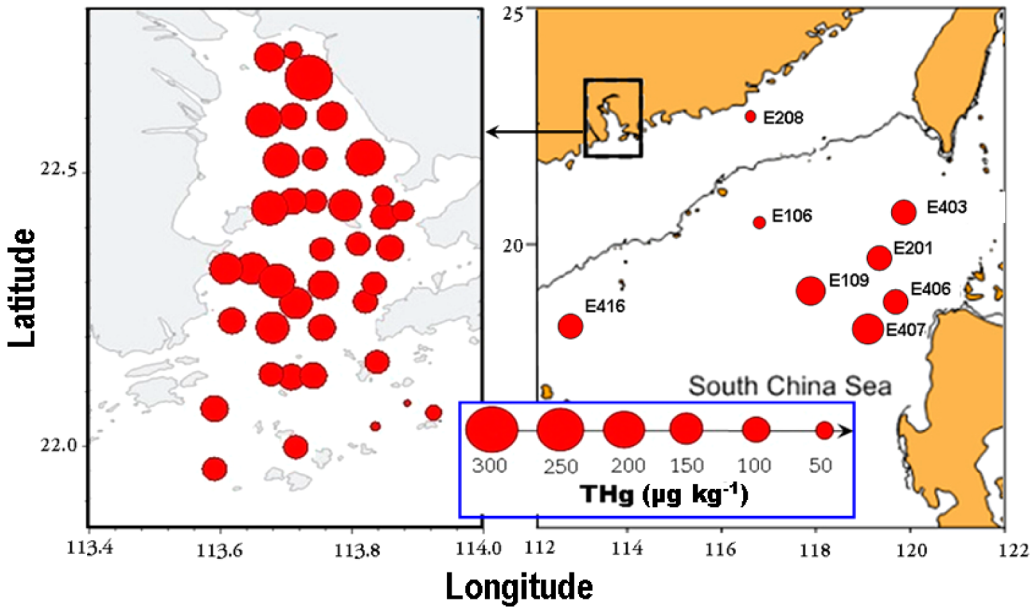

Figure 2. Spatial distribution of THg in the PRE and SCS sediments.

and organic matter (C_{OM}) in the PRE sediments have been reported by Chen et al.[56]

Total Hg (THg) Analysis. Approximately 0.5 g of freeze-dried sediments and standard reference materials (BCR 580, estuarine sediment) were digested using 5 mL of aqua regia (HCl/HNO_3 = 3, v/v) in a water bath (95 °C for 90 min).[11,15,17−19] Ultrapure grades of acid (HNO_3 and HCl) and Mill-Q water (18.2 MΩ cm) were used. After digestion, the solution was centrifuged (3000 rpm for 10 min) at room temperature and then decanted to obtain the supernatant. THg was determined using cold vapor atomic fluorescence spectrometry equipped with a Tekran 2500 Hg analyzer.[57] Quality control was performed using analytical blanks and certified reference material (BCR 580, estuarine sediment). The analytical blanks were lower than <20 pg mL^{-1}. The THg recovery of BCR 580 (126 ± 10 mg kg^{-1}; 2σ; n = 6) was in the range of 91−112%, and the relative variability of sample duplicates was <10%.

Hg Isotopic Composition Analysis. Prior to conducting a Hg isotopic composition analysis, an aliquot solution with a mass of 20 ng of Hg was taken up from each sample digest and diluted to 2 ng mL^{-1} using Milli-Q water. For sample digests with a Hg mass of <20 ng, only 10 ng of Hg was taken up and diluted to 1 ng mL^{-1}. The acid concentrations of the diluted solutions were <20%. Concentrations between the diluted samples and bracketing standards (NIST SRM 3133, in 15% aqua regia) were matched within 10%. The signal for ^{202}Hg was <0.015 V for acid blanks, 0.3−0.4 V for 1 ng mL^{-1} digested solutions, and 0.6−0.7 V for 2 ng mL^{-1} digested solutions, respectively. For sediments with THg < 30 μg kg^{-1} (e.g., sites C5, Y14, E106, and E208), the THg in the digested solutions were too low to conduct Hg isotope analysis. Hence, we will not include these samples in our discussion of Hg isotopic compositions. Hg isotopic compositions were determined using a Nu-Plasma multiple-collector inductively coupled plasma mass spectrometry (MC−ICP−MS). A more detailed description of the overall instrumental setup and analytical conditions used in this study can be found in our previous publications.[58] Hg isotopic variations are reported in δ notation in units of permil (‰) referenced to the NIST SRM 3133 Hg standard (analyzed before and after each sample) using the following equation:[59]

$$\delta^{xxx}\mathrm{Hg}\ (‰) = \{(^{xxx}\mathrm{Hg}/^{198}\mathrm{Hg}_{\mathrm{sample}}) / (^{xxx}\mathrm{Hg}/^{198}\mathrm{Hg}_{\mathrm{NIST\ SRM\ 3133}}) - 1\} \times 1000 \quad (1)$$

where *xxx* is the mass of each Hg isotope between 199 and 202 amu. MIF is reported in capital delta notation ($\Delta^{xxx}Hg$, deviation from mass dependency in units of permil, ‰).[59]

$$\Delta^{199}\mathrm{Hg} \approx \delta^{199}\mathrm{Hg} - (\delta^{202}\mathrm{Hg} \times 0.2520) \quad (2)$$

$$\Delta^{200}\mathrm{Hg} \approx \delta^{200}\mathrm{Hg} - (\delta^{202}\mathrm{Hg} \times 0.5024) \quad (3)$$

$$\Delta^{201}\mathrm{Hg} \approx \delta^{201}\mathrm{Hg} - (\delta^{202}\mathrm{Hg} \times 0.7520) \quad (4)$$

The reproducibility of isotopic data was assessed by measuring replicate sample digests (n = 2). To assess matrix-induced fractionation bias, we ran UM-Almadén standard solutions (diluted in 15% aqua regia) repeatedly with a THg concentration of 1 ng mL^{-1} (n = 3) and 2 ng mL^{-1} (n = 6). The overall average and uncertainty of the δ values for UM-Almadén (δ^{202}Hg, −0.50 ± 0.08‰; Δ^{199}Hg, +0.01 ± 0.03‰; Δ^{200}Hg, +0.02 ± 0.03‰; Δ^{201}Hg, −0.03 ± 0.04‰; 2σ; n = 9) agreed well with those of the previous studies.[59] The uncertainties reported in this study corresponded to the larger value of either the external precision of repeated measurements of the UM-Almadén or the uncertainty from measuring replicate sediment digests. Measurements of replicate digests of BCR 580 (δ^{202}Hg, −0.44 ± 0.08‰; Δ^{199}Hg, −0.03 ± 0.04‰; Δ^{200}Hg, +0.03 ± 0.03‰; Δ^{199}Hg, −0.04 ± 0.04‰; 2σ; n = 6) also agree well with the data reported by Liu et al.[11]

RESULTS AND DISCUSSION

Total Concentration of Hg in Sediments of the PRE and SCS. The concentrations of THg in the PRE and SCS sediments are shown in Table S1 of the Supporting Information. The spatial distribution of THg concentrations

DOI: 10.1021/es504070y
Environ. Sci. Technol. 2015, 49, 1347−1355

(Figure 2) in sediments was characterized by lower concentrations in sediments of the SCS and elevated concentrations at the PRE. The THg in the SCS sediments ranged from 12 to 83 μg kg^{-1}, with a mean value of 60 ± 29 μg kg^{-1} (1σ; n = 8). The THg in the SCS sediments was comparable to the previously measured THg (mean, 61 μg kg^{-1}; n = 53) in the SCS[60] and the background THg (20−100 μg kg^{-1}) in ocean sediments of the world.[61] Atmospheric deposition was considered to be the major pathway for THg entering the open oceans,[3] such as the SCS.[62] Fu et al.[62] investigated the potential sources (e.g., atmospheric Hg deposition versus riverine input) of Hg in the SCS. According to their study, inputs of Hg into the SCS via atmospheric deposition and riverine delivery were estimated to be 9.2 × 10^4 and 3.4 × 10^4 kg year^{-1}, respectively.[62]

The THg in the PRE sediments ranged from 8 to 251 μg kg^{-1}, with a mean value of 94 ± 43 μg kg^{-1} (1σ; n = 39). The THg data in the present study is comparable to data from previous studies conducted in the PRE.[6−9] The concentrations of THg in the PRE sediments showed a pattern of decrease from the northern PRE to the southern PRE (Figure 2). A similar trend for THg in the sediments of the PRE was also observed by Shi et al.[8] As shown in Figure 2, the data on elevated levels of THg were found in sediments located at the northwest part of the PRE, which is close to the mouth of the main stream of the Pearl River. In the PRE region, most cities and industries are sited along the Pearl River. Several studies have demonstrated that riverine transport of domestic and industrial wastewater is the most important source of Hg in the PRE.[6−8] Riverine transport of fine particles has been demonstrated to play an important role in delivering Hg to estuarine sediments.[4,5] Fine particles usually contain a great deal of organic matter (e.g., humic acid, fulvic acid, and amino acids), which has a strong affinity to bind with Hg.[63−65] According to Chen et al.,[56] PRE sediments generally contain relatively high levels of C_{OM} (range, 2.43−6.71%; mean, 4.45%). As shown in panels a and b of Figure 3, positive

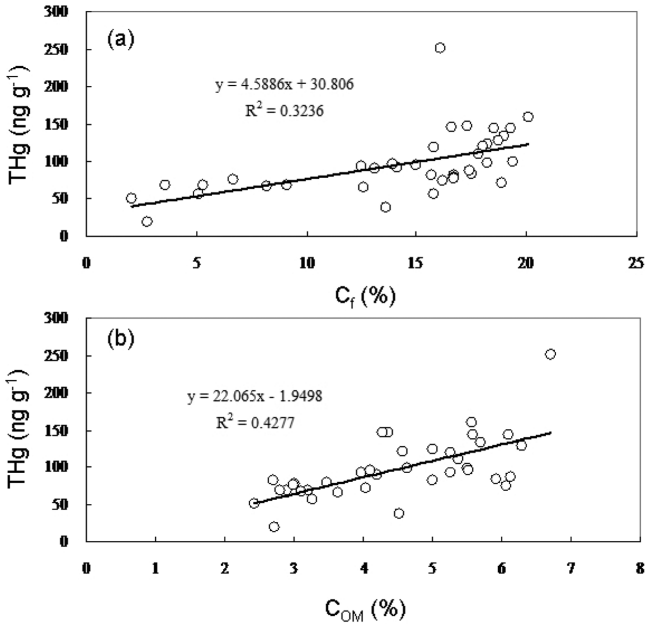

Figure 3. Relation between THg and (a) organic matter content and (b) content of fine particles in the PRE sediments.

correlations were observed between THg and C_f (r^2 = 0.32; p < 0.05) and between THg and C_{OM} (r^2 = 0.43; p < 0.05) in sediments of the northern and middle PRE, suggesting that fine organic particles are the major carriers of Hg in the PRE.[66] As shown in Table S2 of the Supporting Information, THg in the PRE sediments was also significantly correlated with other trace metals (e.g., Co, Cr, Cu, Ni, etc.) (r^2 > 0.50; p < 0.05) reported by Chen et al.,[56] indicating a great influence of industrial activities.

Hg Isotopic Compositions in Sediments in the SCS and PRE. The Hg isotopic compositions in the PRE and SCS sediments are summarized in Table S1 of the Supporting Information. Because of the absence of Hg isotopic data on the low Hg samples (e.g., C5, Y14, E106, and E208), we will not include these samples in our discussion of Hg isotopic compositions. As shown in Figure 4, differences in Hg isotopic

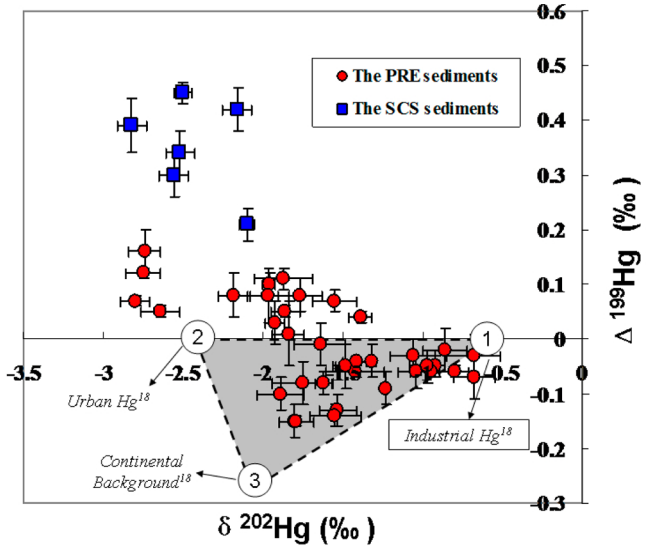

Figure 4. Plot of Δ^{199}Hg versus δ^{202}Hg in the PRE and SCS sediments.

compositions were observed in sediments in the SCS and PRE. For instance, sediments collected from the SCS (excluding sites E106 and E208) showed the most negative δ^{202}Hg values (range, from −2.82 to −2.10‰; mean, −2.44 ± 0.27‰; 1σ; n = 6) and positive Δ^{199}Hg values (range, from +0.21 to +0.45‰; mean, +0.35 ± 0.09‰; 1σ; n = 6). Sediments in the PRE (excluding sites C5 and Y14) showed relatively higher δ^{202}Hg values (range, from −2.80 to −0.68‰; mean, −1.60 ± 0.56‰; 1σ; n = 37) and relatively negative Δ^{199}Hg values (range, from −0.15 to +0.16‰; mean, −0.01 ± 0.08‰; 1σ; n = 37). The variations in the Hg isotopic compositions in sediments of the PRE and SCS may be explained by (1) isotope fractionation of Hg during geochemical cycling and/or (2) the mixing of Hg from different sources with distinct isotope signatures, as discussed below.

Mercury Isotopic Composition in Sediments of the SCS. It has been established that positive Δ^{199}Hg values (range, from +0.21 to +0.45‰; mean, +0.35 ± 0.09‰; 1σ; n = 6) are a feature of the SCS sediments (not including sites E106 and E208). Positive Δ^{199}Hg values have also been observed in coastal sediments in the Central Portuguese Margin (+0.09 ± 0.04‰; 1σ; n = 8),[47] the mid-Pleistocene sapropels from the Mediterranean Sea (+0.11 ± 0.03‰; 1σ; n = 5),[46] and premining sediments in the San Francisco Bay region (+0.17 ±

DOI: 10.1021/es504070y
Environ. Sci. Technol. 2015, 49, 1347−1355

0.03‰; 1σ; n = 5).[51] To our knowledge, the SCS sediments showed the largest positive Δ^{199}Hg values (up to +0.45‰) for oceanic sediments reported thus far. One possible explanation for the large positive Δ^{199}Hg observed in the SCS could be atmospheric Hg deposition, because a previous study by Fu et al.[62] demonstrated that >70% of Hg in the SCS is of atmospheric deposition origin.[62] Large MIF of odd Hg isotopes (e.g., ^{199}Hg and ^{201}Hg) has been reported in precipitation and direct atmospheric Hg samples.[23−27] In general, negative Δ^{199}Hg values were reported in elemental gaseous Hg (Hg^0), while positive Δ^{199}Hg values were reported in gaseous oxidized Hg (Hg^{2+}) and particulate/aerosol-bound Hg (Hg_p) species.[25−27] Precipitations, which mainly contain Hg^{2+} and Hg_p, showed positive Δ^{199}Hg values.[23−25] For instance, Gratz et al.[23] reported positive Δ^{199}Hg (from +0.04 to +0.52‰) in precipitation and negative Δ^{199}Hg (from −0.21 to +0.06‰) in gaseous Hg samples in the Great Lakes region (U.S.A.). Sherman et al.[26] reported negative Δ^{199}Hg (from −0.11 to −0.22‰) in total gaseous Hg in Arctic areas. Rolison et al.[27] reported distinct Δ^{199}Hg in particulate Hg (from +0.36 to +1.36‰), reactive gaseous Hg (Δ^{199}Hg, from −0.28 to 0.18‰), and gaseous elemental Hg (Δ^{199}Hg, from −0.41 to −0.03‰) in the Grand Bay (U.S.A.). The SCS sediments, which have positive Δ^{199}Hg values, may reflect Hg from precipitations and gaseous oxidized Hg (Hg^{2+}) and particulate/aerosol-bound Hg (Hg_p) species.[23−27] It should be noted that previous studies on precipitation and atmospheric Hg species also reported MIF of even Hg isotopes (e.g., ^{200}Hg).[23−27] In general, Hg^0 was characterized by negative Δ^{200}Hg values, while the precipitation and oxidized atmospheric Hg species (which contains Hg^{2+} and Hg_p) mainly displayed positive Δ^{200}Hg values.[23−27] In this study, the absence of the MIF signature of ^{200}Hg in the SCS sediments is consistent with previous studies in ocean sediments,[46−49] which could be explained by the mixing of gaseous elemental mercury (with negative Δ^{200}Hg values) with precipitation and oxidized atmospheric Hg species (with positive Δ^{200}Hg values).[23−27]

Post-depositional MIF processes may also alter the Δ^{199}Hg values in the sediments. On the basis of current knowledge, there are two possible mechanisms for the MIF of Hg: the nuclear volume effect (NVE)[67] and the magnetic isotope effect (MIE).[68] The NVE has been documented during elemental Hg evaporation[39,69] and equilibrium Hg−thiol complexation.[40] Elemental Hg^0 volatilization had a Δ^{199}Hg/Δ^{201}Hg of 1.65−2.0 for NVE.[39,69] Equilibrium Hg−thiol complexation caused NVE with a Δ^{199}Hg/Δ^{201}Hg of 1.54.[40] The MIE has been observed during photoreactions of aqueous Hg,[28,34,35] which showed a different pattern of Δ^{199}Hg/Δ^{201}Hg from the NVE. For instance, experiments show that MeHg photodegradation generates Δ^{199}Hg/Δ^{201}Hg of 1.36, while Hg^{2+} photoreduction generates Δ^{199}Hg/Δ^{201}Hg of 1.00−1.30.[28,34,35] Recent studies by Jackson and associates demonstrated that biochemical-mediated processes, which generated free radicals that produce the same effects as photochemically produced free radicals, may also cause MIF in the aqueous environment.[20−22,29] However, among different processes that cause MIF, photochemical reactions are more likely the cause for the positive Δ^{199}Hg values in the SCS. Photoreduction of aqueous Hg^{2+} driven by natural dissolved organic matter (DOM) resulted in releasing Hg^0 with negative MIF, leaving the remaining Hg^{2+} with positive MIF signatures.[28] As shown in Figure 5, all of the PRE and SCS sediments yielded a Δ^{199}Hg/Δ^{201}Hg of 1.05 ± 0.06 (2σ), which is consistent with that of the photoreduction of

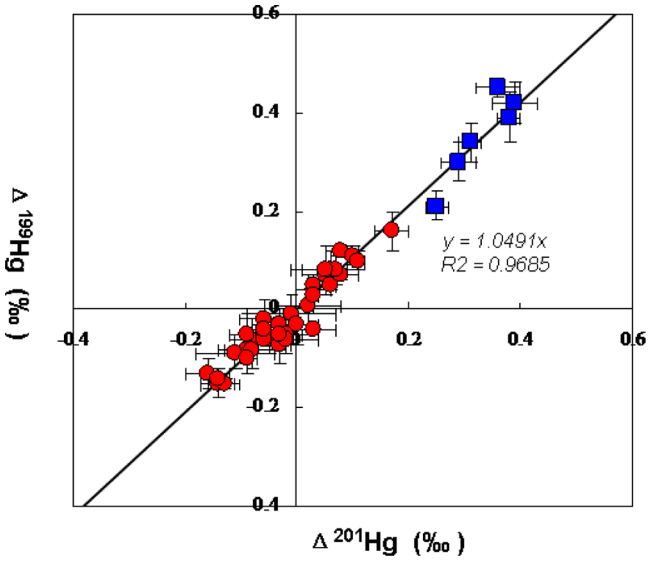

Figure 5. Mass-independent fractionation of Hg isotopes in the PRE and SCS sediments.

Hg^{2+} reported by Bergquist and Blum.[28] In the SCS, much higher water clarities (Sechhi depth > 20 m) and much slower sediment accumulation rates have been reported. The high water clarity can lead to high exposure to sunlight, which may increase the photoreduction of Hg^{2+} in marine waters.[51] If we assume that Hg^{2+} photoreduction experiments conducted by Bergquist and Blum[28] are applicable to the SCS, we estimate that >20% of Hg in the SCS was photoreduced (see the calculation results in the Supporting Information).

We observed the most negative δ^{202}Hg values (mean, −2.44 ± 0.27‰; 1σ; n = 6) in the SCS sediments. The degassing of dissolved Hg^0 and the physical settling of Hg by particles are the two important processes affecting Hg mobility in the water column.[70] The degassing of dissolved Hg^0 could not be the main process causing the lower δ^{202}Hg values in the SCS sediments because volatilization,[38] microbial reduction,[30,31] and photoreduction[28,34,35] processes tend to produce negative δ^{202}Hg in the product Hg^0, which will cause the positive δ^{202}Hg values in the water column. Indeed, relatively higher δ^{202}Hg values (from −0.50 to −1.50‰) have been reported in seawaters compared to the SCS sediments.[71] The physical settling of Hg adsorbed to particles could be the possible cause of the lower δ^{202}Hg values in the SCS. Fractionation of Hg isotopes between aqueous and solid phases has been reported during the binding of Hg with thiol groups,[40] sorption to goethite,[41] and precipitation with sulfides,[72] all of which are processes that can lead to negative δ^{202}Hg values in the solid phase. Another reason for the lower δ^{202}Hg values in the SCS could be the atmospheric deposition of Hg.[62] Although large variations in δ^{202}Hg values have been reported in atmospheric Hg samples;[23−27] however, Blum et al.[44] stated that atmospheric Hg emitted from anthropogenic sources generally have much lower δ^{202}Hg values. For instance, total gaseous Hg collected in the Wanshan Hg mine (southwest China) showed negative δ^{202}Hg from −2.32 to −1.85‰.[73] Gaseous Hg^0 collected near a coal-fired power plant (Grand Bay, U.S.A.) displayed negative δ^{202}Hg from −3.88 to −0.33‰.[27] Precipitation collected close to a coal-fired utility boiler (Crystal River, U.S.A.) also displayed large negative δ^{202}Hg values (mean, −2.56‰; n = 28).[74] Fu et al.[62] demonstrated

DOI: 10.1021/es504070y
Environ. Sci. Technol. 2015, 49, 1347−1355

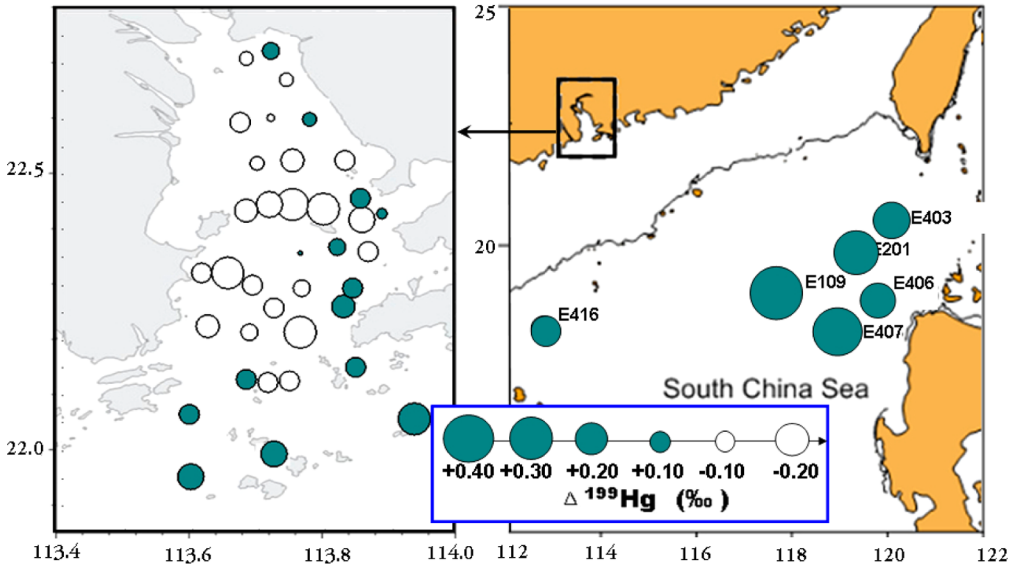

Figure 6. Spatial distribution of Δ^{199}Hg in the PRE and SCS sediments.

that anthropogenic Hg emissions from South China and the Indochina peninsula are the main sources of Hg in the SCS, which may have caused the lower δ^{202}Hg values in the SCS sediments.

Mercury Isotopic Composition in Sediments of the PRE. The PRE sediments (excluding sites C5 and Y14) showed relatively [analysis of variation (ANOVA) test; $p < 0.02$] negative Δ^{199}Hg values (range, from −0.15 to +0.16‰; mean, −0.01 ± 0.08‰; 1σ; $n = 37$) compared to the SCS. Photolysis of Hg^{2+} bound to thiols can lead to negative Δ^{199}Hg values in the residual Hg^{2+} pool.[35] However, on the basis of the Δ^{199}Hg/Δ^{201}Hg ~ 1 for all of the PRE sediments (Figure 5), we assume that the MIF in the PRE sediments is more likely caused by Hg^{2+} photoreduction driven by natural DOM.[28] Previous studies have indicated that the photochemical cycling of Hg can be related to variable exposure to sunlight.[49,51] Because of the input of the Pearl River, very high total suspended matter contents (>34 mg L^{-1}) and sedimentation rates (>1.5 cm $year^{-1}$) have been documented in the PRE[54] and much lower water clarity was observed in the northern PRE (Secchi disk depth < 1 m).[54,55] The lower water clarity would prevent Hg from Hg^{2+} photoreduction and cause the relatively negative Δ^{199}Hg values in the PRE.

In comparison to the sediments of the SCS, those of the PRE had relatively (ANOVA; $p < 0.02$) higher δ^{202}Hg values (mean, −1.60 ± 0.56‰; 1σ; $n = 37$). In comparison to the SCS, the Hg bond to particulate matters may be more relevant to the PRE because of riverine input of a large amount of soil particles. Close association between THg and C_f ($r^2 = 0.32$; $p < 0.05$; Figure 3a) was observed in the PRE sediments, indicating that fine particles played an important role in transporting Hg to the sediments in the PRE.[64,65,70] Because most Hg can be removed by the particulate matters in the PRE, it is expected that there is a small difference in Hg isotopic compositions between Hg in sediments and the contribution sources. River deliveries of Hg from natural soils and industrial and urban sources are the primary Hg inputs to the coastal ecosystems.[11] In a previous study, Liu et al.[11] investigated Hg isotopic compositions in sediments in the Dongjiang River, one of the largest tributaries flowing into the PRE. They demonstrated that there were significant differences in Hg isotopic compositions in three major sources in the PRE, namely, industrial Hg (δ^{202}Hg, −0.60‰; Δ^{199}Hg, 0), urban Hg (δ^{202}Hg, −2.43‰; Δ^{199}Hg, 0), and continental background Hg (δ^{202}Hg, −2.16‰; Δ^{199}Hg, −0.27‰);[11] none of those sources has a positive Δ^{199}Hg value.[11] Specifically, the industrial Hg source (e.g., batteries, paints, explosives, and light bulbs) is mainly produced from Hg mineral deposits that have not previously been exposed on the Earth's surface. This kind of Hg is therefore unlikely to exhibit significant fractionation for Δ^{199}Hg.[11,75] Previous data on Hg ores, sulfide minerals, and refined Hg have shown no evidence of significant MIF (Δ^{199}Hg, ~ 0).[12−15,44,75] Urban Hg is mainly related to combustion of fossil fuels (e.g., coal). Studies on Hg isotopic compositions in Chinese coals[17] have demonstrated a mean Δ^{199}Hg of ~0. Continental background Hg is mainly related to riverine transport of continental natural soils. Negative Δ^{199}Hg values have been reported in continental non-contaminated soils upstream of the Pearl River[11] and in other areas of the world.[15−19,22,76] As shown in Figure 4, most of the PRE sediments are plotted among the Hg isotopic signature of the three end-members proposed by Liu et al.[11] Those sediments are mainly located in the middle and western edge of the PRE, as shown in Figure 6. The absence of positive Δ^{199}Hg values in those samples is consistent with the fact that riverine deliveries of urban and industrial wastes are the most important sources of Hg in the PRE.[6−9]

We also observed that some PRE sediments fall outside of the ternary mixing model suggested by Liu et al. (Figure 4). As shown in Figure 6, those samples with positive Δ^{199}Hg values (mean, +0.08 ± 0.04‰; 1σ; $n = 13$) were mainly located at the southern and eastern edges of the PRE, influenced by marine currents and away from the mouth of the Pearl River (e.g., Beijiang River and Dongjiang River). Much higher water clarities (Secchi disk depth = 4−18 m) and much slower sediment accumulation rates have been reported in those sites.[54,55] On the basis of the study by Bergquist and Blum,[28] we estimate that ~10% of the Hg^{2+} pool in those samples had been photoreduced before being incorporated into sediments (see the calculations in the Supporting Information).

Environmental Implications. Oceanic and coastal areas are sites that are sensitive to Hg pollution and transformation. Understanding the sources and fate of Hg is critical to assessing

DOI: 10.1021/es504070y
Environ. Sci. Technol. 2015, 49, 1347−1355

the environmental risk of Hg in marine ecosystems. Hg isotopes have been successfully used in many case studies to trace the sources of Hg and the processes of their transformation.[11,15,46−52] Distinct Hg isotopic signatures (both δ^{202}Hg and Δ^{199}Hg values) can be observed in oceanic and estuarine areas. In estuaries, such as the PRE, Hg isotopes transported to the sediments could be less fractionated because of the riverine transport of large amounts of suspended organic particles and the strong bonding of Hg to suspended sediments. Hence, it is possible to identify the potential sources of Hg in estuarine sediments using Hg isotopic signatures. Using Hg isotope compositions, we estimate that river deliveries of Hg from natural soils and industrial and urban sources could be the main inputs of Hg to the PRE. However, in the deep ocean bed of the SCS, source-related signatures of Hg isotopes may have been altered by natural geochemical processes (e.g., Hg^{2+} photoreduction and preferential adsorption processes), especially through the deposition by air to the surface of water. We suggest the use of caution in the application of Hg isotopes as tracers in the open ocean far away from the Hg source regions where secondary fractionation processes may obscure original source signatures.

■ ASSOCIATED CONTENT

Supporting Information

Sampling locations, water depth, Hg isotope compositions, and total Hg concentrations of sediments in the PRE and SCS (Table S1), Pearson correlation coefficient matrix between Hg and other metals in surface sediments of the PRE (Table S2), and photoreduction of Hg^{2+} calculations. This material is available free of charge via the Internet at http://pubs.acs.org.

■ AUTHOR INFORMATION

Corresponding Author

*Telephone: 852-2766-6041. Fax: 852-2334-6389. E-mail: cexdli@polyu.edu.hk.

Notes

The authors declare no competing financial interest.

■ ACKNOWLEDGMENTS

This study was supported by a seed collaborative project from the State Key Laboratory of Marine Pollution, the China Basic Research Program (973 Project, 2013CB430000), the Natural Science Foundation of China (41303014 and 41120134005), and the Research Grants Council (RGC) General Research Fund (663112). The authors thank X. M. Liang, X. P. Huang, Z. Shi, and F. Ye of the South China Sea Institute of Oceanology, Chinese Academy of Sciences, for their assistance in the field sampling program. Last but not least, four anonymous reviewers and Dr. Stephan Hug are acknowledged for their constructive comments and useful suggestions that have largely improved the quality of this paper.

■ REFERENCES

(1) Lindqvist, O.; Johansson, K.; Aastrup, M.; Andersson, A.; Bringmark, L.; Hovsenius, G.; Iverfeld, A.; Meili, M.; Timm, B. Mercury in the Swedish environment. *Water, Air, Soil Pollut.* **1991**, *55*, 193−216.

(2) Driscoll, C. T.; Mason, R. P.; Chan, H. M.; Jacob, D. J.; Pirrone, N. Mercury as a global pollutant: Sources, pathways, and effects. *Environ. Sci. Technol.* **2013**, *47*, 4967−4983.

(3) Fitzgerald, W.; Lamborg, C.; Hammerschmidt, C. Marine biogeochemical cycling of mercury. *Chem. Rev.* **2007**, *107*, 641−662.

(4) Amos, H. M.; Jacob, D. J.; Kocman, D.; Horowitz, H. M.; Zhang, Y.; Dutkiewicz, S.; Horvat, M.; Corbitt, E. S.; Krabbenhoft, D. P.; Sunderland, E. M. Global biogeochemical implications of mercury discharges from rivers and sediment burial. *Environ. Sci. Technol.* **2014**, *48*, 9514−9522.

(5) Chester, R. The transport of material to the oceans: Relative flux magnitudes. In *Marine Geochemistry*, 2nd ed.; Chester, R., Ed.; Blackwell Science: Oxford, U.K., 2003; pp 98−134.

(6) Ip, C. C. M.; Li, X. D.; Zhang, G.; Wai, O. W. H.; Li, Y. S. Trace metal distribution in sediments of the Pearl River Estuary and the surrounding coastal area, South China. *Environ. Pollut.* **2007**, *147*, 311−323.

(7) Shi, Q.; Rueckert, P.; Leipe, T. Distribution and contamination assessment of Hg in the sediments of the Pearl River Estuary. *Mar. Environ. Sci.* **2007**, *26*, 553−556 (in Chinese with an English abstract).

(8) Shi, J. B.; Ip, C. C. M.; Zhang, G.; Jiang, G. B.; Li, X. D. Mercury profiles in sediments of the Pearl River Estuary and the surrounding coastal area of South China. *Environ. Pollut.* **2010**, *158*, 1974−1979.

(9) Yu, X.; Li, H.; Pan, K.; Wang, W. X. Mercury distribution, speciation and bioavailability in sediments from the Pearl River Estuary, Southern China. *Mar. Pollut. Bull.* **2012**, *64*, 1699−1704.

(10) National Development and Reform Commission (NDRC). *The Pearl River Delta Reform Development Project Summary (2008−2020)*; NDRC: Beijing, China, 2008.

(11) Liu, J. L.; Feng, X. B.; Yin, R. S.; Zhu, W.; Li, Z. G. Mercury distributions and mercury isotope signatures in sediments of Dongjiang River, the Pearl River Delta, China. *Chem. Geol.* **2011**, *287*, 81−89.

(12) Hintelmann, H.; Lu, S. Y. High precision isotope ratio measurements of mercury isotopes in cinnabar ores using multi-collector inductively coupled plasma mass spectrometry. *Analyst* **2003**, *128*, 635−639.

(13) Smith, C. N.; Kesler, E.; Blum, J. D.; Rytuba, J. J. Isotope geochemistry of mercury in source rocks, mineral deposits and spring deposits of the California Coast Ranges, USA. *Earth Planet. Sci. Lett.* **2008**, *269*, 399−407.

(14) Smith, C. N.; Kesler, E.; Klaue, B.; Blum, J. D. Mercury isotope fractionation in fossil hydrothermal systems. *Geology* **2005**, *33*, 825−828.

(15) Sonke, J. E.; Schaefer, J.; Chmeleff, J.; Audry, S.; Blanc, G.; Dupre, B. Sedimentary mercury stable isotope records of atmospheric and riverine pollution from two major European heavy metal refineries. *Chem. Geol.* **2010**, *279*, 90−100.

(16) Biswas, A.; Blum, J. D.; Bergquist, B. A.; Keeler, G. J.; Xie, Z. Q. Natural mercury isotope variation in coal deposits and organic soils. *Environ. Sci. Technol.* **2008**, *42*, 8303−8309.

(17) Yin, R. S.; Feng, X. B.; Chen, J. B. Mercury stable isotopic compositions in coals from major coal producing fields in China and their geochemical and environmental implications. *Environ. Sci. Technol.* **2014**, *48*, 5565−5574.

(18) Zhang, H.; Yin, R.; Feng, X.; Sommar, J.; Anderson, C. W. N.; Sapkota, A.; Fu, X.-w.; Larssen, T. Atmospheric mercury inputs in montane soils increase with elevation: Evidence from mercury isotope signatures. *Sci. Rep.* **2013**, *3*, 3322.

(19) Feng, X. B.; Foucher, D.; Hintelmann, H.; Yan, H. Y.; He, T. R.; Qiu, G. L. Tracing mercury contamination sources in sediments using mercury isotope compositions. *Environ. Sci. Technol.* **2010**, *44*, 3363−3368.

(20) Jackson, T. A.; Muir, D. C. G. Mass-dependent and mass-independent variations in the isotope composition of mercury in a sediment core from a lake polluted by emissions from the combustion of coal. *Sci. Total Environ.* **2012**, *417−418*, 189−203.

(21) Jackson, T. A. Mass-dependent and mass-independent variations in the isotope composition of mercury in a sediment core from Lake Ontario as related to pollution history and biogeochemical processes. *Chem. Geol.* **2013**, *355*, 88−102.

(22) Jackson, T. A.; Telmer, K. H.; Muir, D. C. G. Mass-dependent and mass-independent variations in the isotope composition of mercury in cores from lakes polluted by a smelter: Effects of smelter

DOI: 10.1021/es504070y
Environ. Sci. Technol. 2015, 49, 1347−1355

emissions, natural processes, and their interactions. *Chem. Geol.* **2013**, *352*, 27−46.
(23) Gratz, L.; Keeler, G.; Blum, J. D.; Sherman, L. S. Isotopic composition and fractionation of mercury in Great Lakes precipitation and ambient air. *Environ. Sci. Technol.* **2010**, *44*, 7764−7770.
(24) Chen, J. B.; Hintelmann, H.; Feng, X. B.; Dimock, B. Unusual fractionation of both odd and even mercury isotopes in precipitation from Peterborough, ON, Canada. *Geochim. Cosmochim. Acta* **2012**, *90*, 33−46.
(25) Demers, J. D.; Blum, J. D.; Zak, D. R. Mercury isotopes in a forested ecosystem: Implications for air-surface exchange dynamics and the global mercury cycle. *Global Biogeochem. Cycles* **2013**, *27*, 222−238.
(26) Sherman, L. S.; Blum, J. D.; Johnson, K. P.; Keeler, G. J.; Barres, J. A.; Douglas, T. A. Mass-independent fractionation of mercury isotopes in Arctic snow driven by sunlight. *Nat. Geosci.* **2010**, *3*, 173−177.
(27) Rolison, J.; Landing, W.; Luke, W.; Cohen, M.; Salters, V. Isotopic composition of species-specific atmospheric Hg in a coastal environment. *Chem. Geol.* **2013**, *336*, 37−49.
(28) Bergquist, B. A.; Blum, J. D. Mass-dependent and -independent fractionation of Hg isotopes by photoreduction in aquatic systems. *Science* **2007**, *318*, 417−420.
(29) Jackson, T. A.; Whittle, D. M.; Evans, M. S.; Muir, D. C. G. Evidence for mass-independent and mass-dependent fractionation of the stable isotopes of mercury by natural processes in aquatic ecosystems. *Appl. Geochem.* **2008**, *23*, 547−571.
(30) Kritee, K.; Blum, J. D.; Johnson, M. W.; Bergquist, B. A.; Barkay, T. Mercury stable isotope fractionation during reduction of Hg(II) to Hg(0) by mercury resistant microorganisms. *Environ. Sci. Technol.* **2007**, *41*, 1889−1895.
(31) Kritee, K.; Blum, J. D.; Barkay, T. Mercury isotope fractionation during reduction of Hg(II) by different microbial pathways. *Environ. Sci. Technol.* **2008**, *42*, 9171−9177.
(32) Rodríguez-González, P.; Epov, V.; Bridou, R.; Tessier, E.; Guyoneaud, R.; Monperrus, M.; Amouroux, D. Species-specific stable isotope fractionation of mercury during Hg(II) methylation by an anaerobic bacteria (*Desulfobulbus propionicus*) under dark conditions. *Environ. Sci. Technol.* **2009**, *43*, 9183−9188.
(33) Kritee, K.; Barkay, T.; Blum, J. D. Mass dependent stable isotope fractionation of mercury during mercury mediated microbial degradation of monomethylmercury. *Geochim. Cosmochim. Acta* **2009**, *73*, 1285−1296.
(34) Zheng, W.; Hintelmann, H. Mercury isotope fractionation during photoreduction in natural water is controlled by its Hg/DOC ratio. *Geochim. Cosmochim. Acta* **2009**, *73*, 6704−6715.
(35) Zheng, W.; Foucher, D.; Hintelmann, H. Isotope fractionation of mercury during its photochemical reduction by low-molecular-weight organic compounds. *J. Phys. Chem. A* **2010**, *114*, 4246−4253.
(36) Yang, L.; Sturgeon, R. E. Isotopic fractionation of mercury induced by reduction and ethylation. *Anal. Bioanal. Chem.* **2009**, *393*, 377−385.
(37) Zheng, W.; Hintelmann, H. Nuclear field shift effect in isotope fractionation of mercury during abiotic reduction in the absence of light. *J. Phys. Chem. A* **2010**, *114*, 4238−4245.
(38) Zheng, W.; Foucher, D.; Hintelmann, H. Mercury isotope fractionation during volatilization of Hg(0) from solution into the gas phase. *J. Anal. At. Spectrom.* **2007**, *22*, 1097−1104.
(39) Estrade, N.; Carignan, J.; Sonke, J. E.; Donard, O. F. X. Mercury isotope fractionation during liquid−vapor evaporation experiments. *Geochim. Cosmochim. Acta* **2009**, *73*, 2693−2711.
(40) Wiederhold, J. G.; Daniel, K.; Infante, I.; Bourdon, B.; Kretzschmar, R. Equilibrium mercury isotope fractionation between dissolved Hg(II) species and thiol-bound Hg. *Environ. Sci. Technol.* **2010**, *44*, 4191−4197.
(41) Jiska, M.; Wiederhold, J.; Bourdon, B.; Kretzschmar, R. Solution speciation controls mercury isotope fractionation of Hg(II) sorption to goethite. *Environ. Sci. Technol.* **2012**, *46*, 6654−6662.
(42) Yin, R. S.; Feng, X. B.; Wang, J. B.; Bao, Z. D.; Yu, B.; Chen, J. B. Mercury isotope variations between bioavailable mercury fractions and total mercury in mercury contaminated soil in Wanshan Mercury Mine, SW China. *Chem. Geol.* **2013**, *336*, 80−86.
(43) Yin, R. S.; Feng, X. B.; Shi, W. F. Application of the stable-isotope system to the study of sources and fate of Hg in the environment: A review. *Appl. Geochem.* **2010**, *25*, 1467−1477.
(44) Blum, J. D.; Sherman, L. S.; Johnson, M. W. Mercury isotopes in Earth and environmental sciences. *Annu. Rev. Earth Planet. Sci.* **2014**, *42*, 249−269.
(45) Yin, R. S.; Feng, X. B.; Li, X. D.; Yu, B.; Du, B. Y. Trends and advances in mercury stable isotope system as a geochemical tracer. *Trends Environ. Anal. Chem.* **2014**, *2*, 1−10.
(46) Gehrke, G. E.; Blum, J. D.; Meyers, P. A. The geochemical behavior and isotopic composition of Hg in a mid-Pleistocene western Mediterranean sapropel. *Geochim. Cosmochim. Acta* **2009**, *73*, 1651−1665.
(47) Mil-Homens, M.; Blum, J. D. Tracing anthropogenic Hg and Pb input using stable Hg and Pb isotope ratios in sediments of the central Portuguese Margin. *Chem. Geol.* **2013**, *336*, 62−71.
(48) Foucher, D.; Ogring, N.; Hintelmann, H. Tracing mercury contamination from the Idrija Mining Region (Slovenia) to the Gulf of Trieste using Hg isotope ratio measurements. *Environ. Sci. Technol.* **2009**, *43*, 33−39.
(49) Gehrke, G. E.; Blum, J. D.; Marvin-DiPasquale, M. Sources of mercury to San Francisco Bay surface sediment as revealed by mercury stable isotopes. *Geochim. Cosmochim. Acta* **2011**, *75* (3), 691−705.
(50) Yin, R. S.; Feng, X. B.; Wang, J. X.; Li, P.; Liu, J. L.; Zhang, Y.; Chen, J. B.; Zheng, L. R.; Hu, T. D. Mercury speciation, mercury isotope fractionation during ore roasting process and their implication to source identification of downstream sediment in Wanshan mercury mining area, SW China. *Chem. Geol.* **2013**, *336*, 87−95.
(51) Donovan, P. M.; Blum, J. D.; Yee, D.; Gehrke, G. E.; Singer, M. B. An isotopic record of mercury in San Francisco Bay sediment. *Chem. Geol.* **2013**, *349*, 87−98.
(52) Jackson, T. A.; Muir, D. C. G.; Vincent, W. F. Historical variations in the stable isotope composition of mercury in Arctic lake sediments. *Environ. Sci. Technol.* **2004**, *38*, 2813−2821.
(53) Ye, L.; Preiffer, K. D. Studies of 2D & 3D numerical simulation of Kelvin tide wave in Nei Lingdingyang at Pearl River Estuary. *Ocean Eng.* **1990**, *8*, 33−44.
(54) Xi, H.; Zhang, Y. Total suspended matter observation in the Pearl River estuary from in situ and MERIS data. *Environ. Monit. Assess.* **2011**, *77*, 563−574.
(55) Chen, L.; Xie, J.; Peng, X.-j.; Li, Z.; Lou, Q.-s.; Zhang, X.-h.; Yang, F. The relationship between seawater clarity and water-leaving reflectance spectra of seawater in the Pearl River Estuary. *Remote Sens. Land Resour.* **2011**, *2011* (23), 151−155 (in Chinese with English abstract).
(56) Chen, B. W.; Liang, X.; Xu, W. H.; Huang, X. P.; Li, X. D. The changes in trace metal contamination over the last decade in surface sediments of the Pearl River Estuary, South China. *Sci. Total Environ.* **2012**, *439*, 141−149.
(57) United States Environmental Protection Agency (U.S. EPA). *Method 1631: Mercury in Water by Oxidation, Purge and Trap, and Cold Vapor Atomic Fluorescence Spectrometry*; Office of Water, U.S. EPA (4303): Washington, D.C., 1999; EPA-821-R-99-005, pp 1−33.
(58) Yin, R. S.; Feng, X. B.; Foucher, D.; Shi, W. F.; Zhao, Z. Q.; Wang, J. High precision determination of mercury isotope ratios using online mercury vapor generation system coupled with multi-collector inductively coupled plasma−mass spectrometer. *Chin. J. Anal. Chem.* **2010**, *38*, 929−934.
(59) Blum, J. D.; Bergquist, B. A. Reporting of variations in the natural isotopic composition of mercury. *Anal. Bioanal. Chem.* **2007**, *388*, 353−359.
(60) Zhang, Y.; Du, J. Background values of pollutants in sediments of the South China Sea. *Acta Oceanol. Sin.* **2005**, *27*, 161−166 (in Chinese with an English abstract).

DOI: 10.1021/es504070y
Environ. Sci. Technol. 2015, 49, 1347−1355

(61) Lindqvist, O.; Jernelov, A.; Johansson, K.; Rohde, H. *Mercury in the Swedish Environment. Global and Local Sources*; National Swedish Environmental Protection Board: Stockholm, Sweden, 1984.
(62) Fu, X. W.; Feng, X. B.; Zhang, G.; Xu, W. H.; Li, X. D.; Yao, H.; Liang, P.; Li, J.; Sommar, J.; Yin, R. S.; Liu, N. Mercury in the marine boundary layer and seawater of the South China Sea: concentrations, air/sea flux, and implication for land outflow. *J. Geophys. Res.* **2010**, *115*, D06303.
(63) Ramalhosa, E.; Pato, P.; Monterroso, P.; Pereira, E.; Vale, E.; Duarte, A. C. Accumulation versus remobilization of mercury in sediments of a contaminated lagoon. *Mar. Pollut. Bull.* **2006**, *52*, 332−356.
(64) Berto, D.; Giani, M.; Covelli, S.; Bosc, R.; Cornello, M.; Macchia, S.; Massironi, M. Mercury in sediments and *Nassarius reticulatus* (Gastropoda, Prosobranchia) in the southern Venice Lagoon. *Sci. Total Environ.* **2006**, *368*, 298−305.
(65) Skyllberg, U.; Bloom, P. R.; Qian, J.; Lin, C. M.; Bleam, W. F. Complexation of mercury(II) in soil organic matter: EXAFS evidence for linear two-coordination with reduced sulfur groups. *Environ. Sci. Technol.* **2006**, *40*, 4174−4180.
(66) Liu, J. L.; Feng, X. B.; Zhu, W.; Zhang, X.; Yin, R. S. Distribution and speciation of mercury and methyl mercury in surface water of Dongjiang River, the Pearl River Delta, China. *Environ. Sci. Pollut. Res.* **2012**, 2012.
(67) Schauble, E. A. Role of nuclear volume in driving equilibrium stable isotope fractionation of mercury, thallium, and other very heavy elements. *Geochim. Cosmochim. Acta* **2007**, *71*, 2170−2189.
(68) Buchachenko, A. L.; Lukzen, N. N.; Pedersen, J. B. On the magnetic field and isotope effects in enzymatic phosphorylation. *Chem. Phys. Lett.* **2007**, *434*, 139−143.
(69) Ghosh, S.; Schauble, E. A.; Lacrampe Couloume, G.; Blum, J. D.; Bergquist, B. A. Estimation of nuclear volume dependent fractionation of mercury isotopes in equilibrium liquid−vapor evaporation experiments. *Chem. Geol.* **2013**, *336*, 5−12.
(70) Laurier, F.; Mason, R.; Whalin, L.; Kato, S. Reactive gaseous mercury formation in the North Pacific Ocean's marine boundary layer: A potential role of halogen chemistry. *J. Geophys. Res.* **2003**, *108* (D17), 4529.
(71) Štrok, M.; Hintelmann, H.; Dimock, B. Development of pre-concentration procedure for the determination of Hg isotope ratios in seawater samples. *Anal. Chim. Acta* **2014**, *851*, 57−63.
(72) Foucher, D.; Hintelmann, H.; Al, T. A.; MacQuarrie, K. T. Mercury isotope fractionation in waters and sediments of the Murray Brook mine watershed (New Brunswick, Canada): Tracing mercury contamination and transformation. *Chem. Geol.* **2013**, *336*, 87−95.
(73) Yin, R. S.; Feng, X. B.; Meng, B. Stable mercury isotope variation in rice plants (*Oryza sativa* L.) from the Wanshan mercury mining district, SW China. *Environ. Sci. Technol.* **2013**, *47*, 2238−2245.
(74) Sherman, L. S.; Blum, J. D.; Keeler, G. J.; Demers, J. D.; Dvonch, J. T. Investigation of local mercury deposition from a coal-fired power plant using mercury isotopes. *Environ. Sci. Technol.* **2012**, *46*, 382−390.
(75) Wiederhold, J. G.; Smith, R. S.; Siebner, H.; Jew, A. D.; Brown, G. E.; Bourdon, B.; Kretzschmar, R. Mercury isotope signatures as tracers for Hg cycling at the New Idria Hg Mine. *Environ. Sci. Technol.* **2013**, *47*, 6137−6145.
(76) Feng, X. B.; Yin, R. S.; Yu, B.; Du, B. Mercury isotope variations in surface soils in different contaminated areas in Guizhou Province, China. *Chin. Sci. Bull.* **2013**, *58*, 249−255.

DOI: 10.1021/es504070y
Environ. Sci. Technol. 2015, 49, 1347−1355